First order magneto-structural phase transition in various functional materials

S. B. Roy and P. Chaddah*

Low Temperature Physics Laboratory, Centre for Advanced Technology, Indore 452 013, India

First order magneto-structural transition plays an important role in the functionality of various magnetic materials of current interest. Rare-earth manganese oxide systems showing colossal magnetoresistance and $Gd_5(Ge,Si)_4$ alloys showing giant magnetocaloric effect are typical examples of such functional materials. The key features of this magneto-structural transition in these two quite distinct types of materials are phase-coexistence and metastability. We highlight this generality by comparing the experimental results with those obtained in another class of magnetic materials. A generalized framework of disorder broadened first order phase transition is introduced to understand the interesting experimental results which have some bearing on the functionality of the concerned materials.

IN recent times various systems with competing ordering are drawing much attention due to their novel physical properties and the associated interesting functionality. One prominent class of materials is transition metal oxides wherein strong electron–electron interaction and electron-lattice interaction give rise to wide ranging phenomena such as exotic magnetic and charge ordering, metal–insulator transition and superconductivity. Magnetoresistance, the change in electrical resistance with an applied magnetic field, is a useful tool in several areas of technology and much of the interest in the rare-earth Mn-oxides is stimulated from the possible utility of the colossal magnetoresistance (CMR) observed in these materials[1,2]. It is now generally recognized that magneto-structural phase transition plays a crucial role in the CMR observed in these Mn-oxide systems[2]. Another class of magnetic materials of current interest is $Gd_5(Ge, Si)_4$ showing giant magnetocaloric effect[3]. They hold much promise for energy efficient and environment friendly magnetic refrigeration. In addition, $Gd_5(Si, Ge)_4$ compounds show giant magnetoelasticity and giant magnetoresistance also[3]. It is now becoming apparent that in this class of materials too magneto-structural transition plays an important role in the observed functionality[4,5]. In this article we show that many features associated with the magneto-structural phase transition in these two quite distinct types of material systems are quite general in nature. Comparing with the results obtained in a test-bed magnetic system namely $CeFe_2$ alloys (which belong to an entirely different class of materials), we shall highlight that the key features associated with such magneto-structural transitions are phase-coexistence and metastability. Further we show that these features are universal characteristics of a disorder-influenced first order phase transition (FOPT). Various novel experimental features reported for CMR-Mn-oxides[2] and magnetocaloric materials[5] $Gd_5(Ge, Si)_4$ can actually be understood in terms of phase-coexistence and metastability. Long range elastic interactions play an important role in such materials and this resolves the apparent contradiction with the Gibbs phase rule in observing phase coexistence over a finite temperature/field regime[6]. A generalized framework of disorder influenced FOPT[7] can be a useful starting point to understand the phase coexistence phenomenon which has now turned out to be an essential feature in the Mn-oxides and has a great influence over the observed CMR in these materials[2].

*For correspondence. (e-mail: chaddah@cat.ernet.in)

Magneto-structural transition in Mn-oxide compounds showing CMR

One of the earliest reports of transition from metallic ferromagnetic (FM) state to insulating charge ordered (CO) antiferromagnetic (AFM) state related to the Mn-oxide system[8] $La_{1/2}Ca_{1/2}MnO_3$. The charge ordered state is characterized by a real space ordering of nominally Mn^{3+} and Mn^{4+} species. On decreasing temperature (T), magnetization (M) drops sharply at the FM–AFM transition temperature (T_N) and the resistivity (ρ) changes by several orders of magnitude. Both $M(T)$ and $\rho(T)$ show thermal hysteresis across T_N and these were taken as an indication of the first order nature of this transition[8]. According to the Ehrenfest classification of phase transitions, a first-order phase transition is accompanied by a discontinuity in the first derivative of the free energy, taken with respect to the control variables that can cause the phase transition. In case the control variables are T and magnetic field (H), one can identify a FOPT if one observes a discontinuous change in entropy (i.e. measure of latent heat) or a discontinuous change in M, as one crosses this transition line by varying either T or H. The FOPT would be firmly established if the magnetization jump and the latent heat satisfy the Clausius–Clapeyron relation. These stringent requirements pose experimental difficulties when the latent heat

is small[9]. In such cases the characteristic feature of hysteresis in a physical property which varies sharply between the two phases, is used to identify a FOPT[9]. In the vicinity of the AFM–FM transition of $La_{1/2}Ca_{1/2}MnO_3$ a drastic change in lattice constants was also observed which was attributed to an incommensurate-to-commensurate charge-ordering transition[10]. Similar first order magneto-structural FM–AFM transition has also been observed[11] in $Nd_{1/2}Sr_{1/2}MnO_3$. Within the AFM state an AFM–FM transition can be induced with the application of an external magnetic field H. This H-induced metamagnetic transition is marked with sharp changes and accompanying hysteresis in various physical properties[2,12]. A (H, T) phase diagram was obtained for $Nd_{1/2}Sr_{1/2}MnO_3$ highlighting a hysteretic region around the $T_C(H)$ line which broadened with decrease in T[2,12].

This FM (metallic)–AFM (charge ordered-insulating) transition in various Mn-oxide systems has been a subject of extensive experimental scrutiny[13–17] which amongst other things has also revealed the electric field-induced change of the charge ordered state[14,16]. Detailed discussion of all these interesting results, however, is beyond the scope of the present review and only a few key experimental observations concerning the magneto structural AFM–FM transition in various Mn-oxide systems are enumerated below: (For detailed information on CMR Mn-oxides the readers are referred to the excellent review by Dagotto *et al.*[2]).

(1) The AFM–FM transition is marked with sharp changes in various physical properties (e.g. magnetization, resistivity, etc.) both in T and H varying measurements and is accompanied with marked hysteresis[2,8,11,12].
(2) The extent of hysteresis in the T-dependent measurements broadens with increase in the (constant) applied field[11,12]. On cooling across T_N in presence of an applied H in various Mn-oxide systems it is possible to retain the FM state (at least in part) in the T regime well below T_N and this is termed as field annealing of the FM state[18,19].
(3) On closer inspection a finite width of the transition is clearly visible. In field-induced transition, magnetization shows changes in the form of distinct steps[20,21].
(4) There is a structural change accompanying this FM–AFM transition[2,10,11].
(5) There exists clear evidence of phase coexistence across the transition and this is elaborated below.

While the phenomenology of the CMR effect in the Mn-oxide systems can be explained within the framework of double exchange interaction, this mechanism alone is insufficient to explain the observed effects quantitatively[2]. A prospective picture in this regard is the formation of a percolation path involving the metallic FM phase in the phase-coexistence regime across the AFM–FM transition which can be manipulated by the applied magnetic field[22,23]. Hence this AFM–FM transition region has been a subject of much scrutiny in recent times using various techniques including microscopic imaging with electron microscopy[24] and magnetic force microscopy[25]. Distinct phase-coexistence on micrometer scale has been reported[24] leading to visualization of a percolating path[25]. Such phase-coexistence on the micrometer scale has been rationalized within the framework of a disorder-influenced first order transition[2,22,23]. In addition, the lattice distortions and long-range strains are known to be important for Mn-oxides[10,26] and the intrinsic complexity of system with strong coupling between electronic and elastic degrees of freedom introduces further interesting features in phase-coexistence[27,28].

Many of these Mn-oxide systems show additional interesting features in the low temperature regime well below T_N. In this low temperature regime the H-induced FM state remains frozen even on withdrawal of the applied field while at higher T the FM–AFM transition is completed at a finite H in the field decreasing cycle. This behaviour is visible both in magnetization[29] and magnetotransport[11] measurements. In magnetization study this gives rise to an anomalous situation where the virgin magnetization curve obtained from the initial zero field cooled state lies outside the envelope magnetization curve obtained in the subsequent field cycling[29].

Magneto-structural transition in Gd_5Ge_4 showing giant magnetocaloric effect

At the origin of the interesting properties in $Gd_5(Ge, Si)_4$ compounds is a magneto-structural transition and we elaborate this below with the results obtained in the parent compound Gd_5Ge_4. This compound has the complex Sm_5Ge_4-type orthorhombic structure at room temperature and it orders antiferromagnetically[5] at $T_N \sim 130$ K. In magnetic fields lower than 10 kOe, this AFM order is sustained at least down[5] to 2 K. Under applied H exceeding 10 kOe (the precise field value is temperature dependent), Gd_5Ge_4 shows interesting AFM–FM transition that could be driven both by T and H and a detailed H–T phase diagram for Gd_5Ge_4 has been obtained through a series of magnetization and heat capacity measurements[5]. High resolution X-ray powder diffraction experiments performed *in situ* under applied H up to 35 kOe have shown that the AFM–FM transition in Gd_5Ge_4 is coupled to a structural transition in which the low H-low T Sm_5Ge_4-type structure transforms to a Gd_5Si_4-type orthorhombic structure[4]. Various other experimental features enumerated above for Mn-oxides are observed in Gd_5Ge_4 and the crucial role of the first order magneto-structural AFM–FM transition in the observed giant magnetocaloric effect in this compound is now well recognized[3–5]. Magneto-thermal hysteresis is one of the numerous evidences pointing towards the first order nature of this transition[5]. Step-like features in the magnetization measurements across the H induced AFM–FM transition have been observed and the commonality with the Mn-oxide systems has been noted[20]. Although phase-coexistence is

an expected feature across this first order AFM–FM transition[5] in Gd_5Ge_4, no imaging study in the line of Mn-oxide materials is reported to date. It should be noted here that unlike in Mn-oxides, the AFM state in Gd_5Ge_4 is metallic in nature.

Below 20 K the conversion of the field-induced FM state to the AFM state in the field reduction cycle becomes sluggish and at 5 K and below, the FM state remains even on reducing H to zero. The initial zero field cooled AFM state, however, can be recovered by heating the sample above 20 K and cooling it down in field <10 kOe. As was in the case of Mn-oxide samples[29], such a behaviour gives rise to the anomalous situation of virgin magnetization curve lying outside the envelope magnetization curve[5].

Magneto-structural transition in doped-$CeFe_2$ alloys: phase-coexistence and metastability

Taken together, many common experimental features from these quite distinct types of materials systems – CMR Mn-oxide materials and giant magnetocaloric material Gd_5Ge_4 are indications of a common underlying physics at least at the phenomenological level. With the benefit of hindsight, we believe that the disorder-influenced first order phase transition provides the basic framework to understand the wide varieties of experimental results in Mn-oxides and Gd_5Ge_4. This idea of generality is mainly developed on the basis of experimental works performed by us on another class of magnetic materials, namely doped-$CeFe_2$ alloys, which are quite different from Mn-oxides and Gd_5Ge_4. These relatively simple doped $CeFe_2$ alloys have been used as a test-bed materials system to study in some details a first order FM–AFM transition. It will be shown here that the key features associated with the AFM–FM transition in Mn-oxides and Gd_5Ge_4 (enumerated above) are clearly observed in this system and that these are a consequence of phase-coexistence and metastability arising out of a disorder-influenced FOPT. In certain H–T regime this FM–AFM transition process is kinetically hindered which also gi ves rise to anomalous experimental features.

$CeFe_2$ is a cubic Laves phase ferromagnet (with Curie temperature $\approx$ 230 K), in which small substitution (< 10%) of selected elements such as Co, Al, Ru, Ir, Os and Re can induce a low temperature AFM state with higher resistivity than the FM state[30,31]. However, unlike in Mn-oxides the AFM state remains a metallic state. A giant magnetoresistance effect[32] associated with the AFM–FM transition is well documented. Neutron diffraction studies on these doped-$CeFe_2$ samples revealed a discontinuous change of the unit cell volume, at the FM–AFM transition, confirming that it is first order[33]. These well characterized Al, Ru and Ir-doped $CeFe_2$ alloys have been used for a detailed study of FOPT[34–39].

The FM–AFM transition in $CeFe_2$ alloys has been studied in detail with ac-susceptibility[30,31,34], resistivity[30,31,36,37,39] and dc magnetization[35–39]. Figure 1 shows M vs T plot for a 4% Ru-doped $CeFe_2$ sample in an applied field of 20 kOe. Three different measurement protocols were used: zero-field cooled (ZFC), field-cooled cooling (FCC) and field-cooled warming (FCW). The paramagnetic (PM)-FM transition is marked by the rapid rise of M with decreasing T below ~210 K and it is thermally reversible. The FM–AFM transition is marked by the sharp drop in M below 50 K and shows substantial thermal hysteresis, which is necessarily a signature of FOPT. It should be noted that the FCC curve does not merge with the ZFC curve down to the lowest measured temperature of 5 K. Similar measurements with applied fields varying between 100 Oe and 30 kOe show that thermal hysteresis broadens with increasing H, and when $H \geq 15$ kOe the M_{FCC} (T) and M_{ZFC} (T) curves fail to merge. $M_{ZFC} \neq M_{FC}$ is an essential feature of the spin-glasses below the spin-glass transition temperature[40] and is termed as thermomagnetic irreversibility (TMI). However, the TMI in spin-glasses collapse with increase in applied H unlike in the present case. Further, it will be shown below that in contrast with the equilibrium field cooled state of spin-glass, here the field cooled state below the transition is a metastable state. As mentioned above very similar increase in hysteresis with applied H has been observed across FM–AFM transition in CMR Mn-oxide systems[41]. Figure 2 shows the schematic H–T phase diagram based on our magnetization measurements with T_{NW}(T_{NC}) as the temperature of the sharp rise (fall) in M in the ZFC (FCC) cycle (see inset of Figure 2). T_{NC} is more precisely defined as the temperature where dM/dT in the M vs T plot changes sign from negative to positive. T^* is the low T point, where M_{ZFC} and M_{FC} merges and T^{**} is the high T counterpart. T^{**} and T_{NC} appear almost the same in our present magnetization measurements. Similar H–T phase diagram can be obtained through transport measurements and in such measurements (under same experimental protocol) T^{**} and T_{NC} can be distinguished clearly[39]. Note that T_{NW}

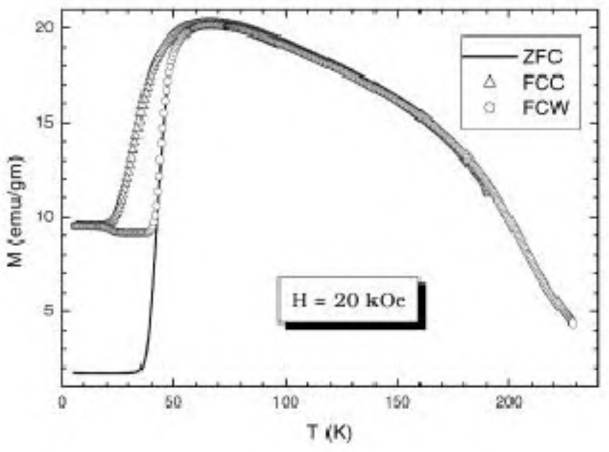

Figure 1. M vs T plots for Ce $(Fe_{0.96}Ru_{0.04})_2$ alloy measured in ZFC, FCC and FCW protocols in an applied field[39] of 20 kOe.

$(H) < T_{NC}(H)$, i.e. the onset of nucleation of the AFM state on cooling occurs at a higher temperature than does nucleation of the FM phase during warming; this indicates that we are dealing with a disorder-broadened first order transition. Such disorder-influenced broadening is observed in the same sample in the field-induced transition as well, and this is discussed in detail in ref. 38. Figure 3 shows schematic curves of the free energy density expressed in terms of an order parameter S as $f(T, S) = (r/2)S^2 - wS^3 + uS^4$ for a first order transition, where w and u are positive temperature independent constants. At $T = T_N$ the high-T and low-T phases coexist. The standard treatment[42] assumes that $r(T) = a[T - T^*]$, where a is positive and temperature independent, and where d^2f/dS^2 at $S = 0$ vanishes at $T = T^*$. The limit of metastability on cooling is reached[42] at $T^* = T_N - w^2/(2ua)$, but finite energy fluctuations can destroy the supercooled state above T^*. Similarly T^{**} is the limit of metastability while heating. In the low temperature AFM regime, a transition from the zero field AFM state to FM state can be induced by application of H[35–39]. As in the case of temperature variation this field-induced first order AFM–FM transition is also marked by distinct hysteresis and phase-coexistence[35–39] and accordingly the limits of metastability H^* and H^{**} can be defined[38]. We find that the sector of the (H, T) diagram in Figure 2 bounded by the $T_{NC}(H)$ and $T^*(H)$ lines is indeed metastable in nature and susceptible to fluctuations (see below).

Figure 2 shows that it is possible to retain residual FM state in this 4% Ru-doped $CeFe_2$ alloy down to the lowest T of measurements by following the FCC path with applied $H \geq 15$ kOe. This is exactly what is termed as field annealing of FM state in various CMR Mn-oxide systems[18,19]. It will now be shown that such FM state obtained by this FCC path is actually metastable in nature. First an isothermal M-H curve is drawn in the ZFC state at 5K by field cycling between 0 and 30 kOe. A distinct 'end point memory' is observed for this M–H curve, namely on completion of the field cycles, the same end point magnetization value is obtained at 30 kOe (see Figure 4). This clearly shows that the magnetic state is stable with respect to any field cycling. On the other hand, isothermal M–H curve obtained after field cooling to 5 K in a field of 30 kOe, shows a distinct lack of 'end point memory' just after a small cycle of reducing the field to 20 kOe and back to 30 kOe (see Figure 4). The difference in the end point magnetization increases with the successive field cycling with increasing amplitude and reaches a maximum value after a complete cycle to 0 Oe and back to 30 kOe. Any subsequent field excursion, however, retains the 'end point memory'. This clearly shows that the residual FM obtained

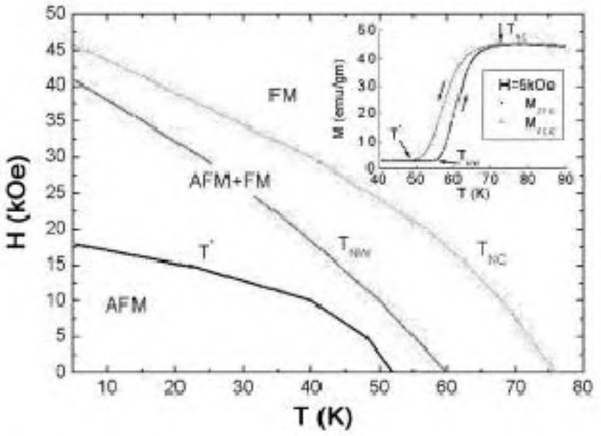

Figure 2. H–T phase diagram for Ce $(Fe_{0.96}Ru_{0.04})_2$ alloy representing T_{NW}, T_{NC} and T^* as a function of H. T_{NC} (T_{NW}) is marked as the point where $M(T)$ shows a rapid rise (fall) while warming up (cooling down). T^* is the temperature where the $M_{ZFC}(T)$ and $M_{FCC}(T)$ curves meet at the low temperature end (see inset). The value of T^* goes below 5 K (our lowest limit) when $H > 15$ kOe.

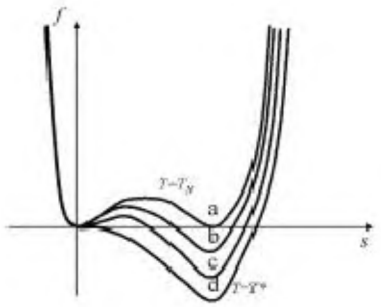

Figure 3. Schematic free energy curves for $T^* < T < T_N$. The high temperature state remains in a local minimum and is stable against infinitesimal energy fluctuations in this temperature regime. The barrier height between the minima corresponding to the high and low temperature phases at T_N (curve a) decreases with the decrease in T and goes to zero at T^* (curve d).

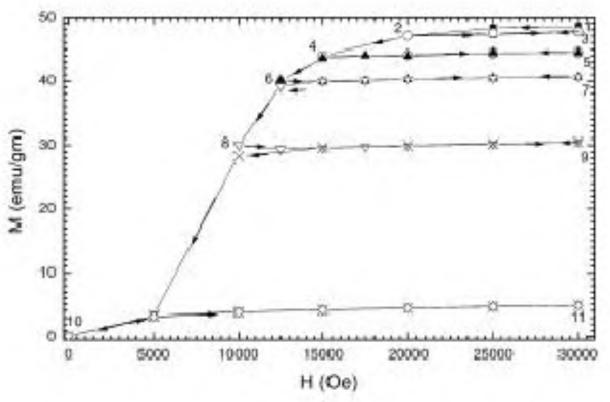

Figure 4. M–H curves drawn for Ce $(Fe_{0.96}Ru_{0.04})_2$ alloy at 5K after field cooling in 30 kOe in the following successive cycles. H = 30 kOe → 20 kOe (path 1–2), 20 kOe → 30 kOe (path 2–3), 30 kOe → 15 kOe (path 3–4), 15 kOe → 30 kOe (path 4–5), 30 kOe → 12.5 kOe (path 5–6), 12.5 kOe → 30 kOe (path 6–7), 30 kOe → 10 kOe (path 7–8), 10 kOe → 30 kOe (path 8–9), 30 kOe → 0 kOe (path 9–10), 0 kOe → 30 kOe (path 10–11). Note the distinct lack of 'end point memory' at the end of each cycling path. Any further cycling after path 10–11 between 0 and 30 kOe traverses the same path reversibly[39].

by the FCC path is very much metastable in nature and can be erased by field cycling. This kind of behaviour is in striking contrast with the nonequlibrium behaviour of spin-glasses, hard ferromagnets and hard superconductors, where the magnetization hysteresis loops always show 'end point memory'.

All these observations can be understood in terms of supercooling of the FM state. While cooling across the first order FM–AFM transition, some amount of the FM state will supercool into the T regime well below the transition line. It is clear from Figure 2 that with applied $H < 15$ kOe the supercooled FM state will cease to exist below a finite T and one can reach the stable AFM state. This is indicated by the merger of the FC and ZFC magnetization. With $H \geq 15$ kOe some amount of supercooled FM state remains down to the lowest T of measurement. As a result, FC magnetization always remains higher than the ZFC counterpart in the temperature regime below the FM–AFM transition. The region between $T_{NC}(H)$ and $T^*(H)$ line in Figure 2 marks the phase-coexistence region formed during the cooling path. At the onset of the FM–AFM transition, the regions with AFM ordering will start nucleating and the nucleation will be complete at the $T^*(H)$ line. The phase-coexistence region consists of mixtures of AFM and FM clusters and it is metastable in nature. A 'minor hysteresis loop technique' developed earlier in the context of vortex matter phase transition[43] has been used to study the phase coexistence across the FM–AFM transition[34,35]. The lack of 'end point memory' effect, as mentioned above, is a consequence of such metastability. On drawing a M–H curve in this metastable phase-coexistence region (obtained via FCC path) one introduces energy fluctuations, which drive the clusters of metastable FM state to the stable AFM state. Further support of metastable nature of the phase-coexistence state has come from large relaxation of both magnetization and resistivity in the phase-coexistence regime[38,44]. Large relaxation behaviour is a characteristic feature of the phase-coexistence state in Mn-oxides[45].

The question remains whether a superheated regime of the AFM state also exists in the H–T phase space of the present sample. Traditionally, superheating is relatively difficult to observe. However, some preliminary 'end point memory' tests indicate the presence of metastability in the H–T regime in Figure 2 between T_{NW} and the $T^{**}(H)$ line[44]. In addition, large magnetization relaxation is observed in the same (H, T) region, which indicates the presence of superheated AFM state[38].

Disorder-influenced first order phase transition

The composition in any alloy or doped compound varies around some average composition due to the disorder that is frozen in as the solid crystallizes from the melt. It was proposed earlier[7] that such static, quenched in, purely statistical compositional disorder can, under certain circumstances, introduce a landscape of transition temperatures in a system undergoing first order phase transition. Detailed computational studies[22,23] confirm the applicability of such a picture in CMR Mn-oxide compounds. According to some computer simulations and mean field approximations, the FM and AFM-CO phases are separated by FOPT when models without disorder are used. Intrinsic quenched disorder smears this FOPT, introduces phase-coexistence and effectively transforms the FOPT into a quasi-continuous transition with percolative characteristics. Such studies further emphasize that phase-coexistence can occur in any system in the presence of quenched disorder whenever two states are in competition through a first order phase transition[2]. Such intrinsic disorder induced landscape of transition temperatures/fields has actually been observed across the vortex solid melting transition in a high temperatures superconductor BSCCO[46]. The applicability of such a picture in the AFM–FM transition of the doped-$CeFe_2$ alloys has been pointed out through an imaging study using a micro Hall probe[47]. It was observed both in T and H variation measurements that the FM clusters of various sizes appear in random positions of the sample at the onset of the AFM–FM transition. As the temperature or field is increased, new FM clusters appears until the whole sample is converted into the FM state. This is indicative of the local variation of the AFM–FM transition temperature (T_N) or field (H_M) leading to a rough T_N/H_M landscape. This distribution of T_N or H_M gives rise to the impression of a global rounding of the transition in bulk measurements. On reducing the temperature or field from well inside the FM state, FM clusters are seen to exist in the T or H regime, where, in the T or H increasing cycle, the sample was in the equilibrium AFM state. This is a visual proof of supercooling of the FM state across the AFM–FM transition and such supercooled state can easily be destabilized with a small energy fluctuation. In the less disordered samples the growth process of the clusters is relatively fast with smaller number of nucleating clusters, which suggests that different disorder landscapes can control nucleation and growth with the key point that if the growth is slow enough, percolation will occur over an observable T or H interval before phase-coexistence collapses. Such percolative behaviour can be controlled by subtle changes in sample doping, and the ramification to tuning the functionality of the Mn-oxide systems, for example, is obvious[47].

The clusters in the phase-coexistence regime of doped-$CeFe_2$ alloys have a size distribution in the range of 5–100 microns. This is somewhat larger than the length scale of 0.5 micron observed in CMR Mn-oxides[2,24] and discussed in the existing theories[22,23]. However, the issue of phase-coexistence has become even more interesting recently with the possible coupling between electronic and elastic degrees of freedom which can give rise to phase-coexistence in even larger scale[27,28]. This recent development is very much relevant for the FM–AFM transition in doped $CeFe_2$ alloys which is accompanied by a cubic to

rhombohedral structural distortion[33]. This magneto-structural coupling in doped-$CeFe_2$ alloys probably plays an important role in certain anomalous low temperature properties which are particularly visible in Al-doped $CeFe_2$ alloys. In these alloys below 20 K the field-induced FM state does not revert completely to the AFM state on withdrawal of the applied field[36,37]. This gives rise to the striking feature of the ZFC virgin M–H curve lying out of the envelope M–H curve obtained by subsequent field cycling between H_{max}, where $H_{max} \gg H_M$ (see Figure 5). This anomalous feature is reflected in the field dependence of resistivity as well[37]. As mentioned, earlier similar behaviour has been observed in CMR Mn-oxides[11,29] and magnetocaloric materials[5]. As a possible explanation of the observed anomalous features we introduce the idea that the kinetics of the FM to AFM transition gets arrested at low T and in high H[36,37]. We recognize that for (H, T) values below (H^*, T^*) line, the free energy barrier separating the FM from the AFM phase has dropped to zero throughout the sample. An infinitesimal fluctuation should drive any FM region to the AFM phase. But all our observations indicate that at very low T the (unstable) FM regions remain in the AFM phase. It is well known that at sufficiently low T the characteristic time for structural relaxation becomes larger than experimental time-scales[48]. We postulate that at sufficiently low T the displacive motion of atoms involved in the structural distortion that is associated with the FM–AFM transition in Al-doped $CeFe_2$ samples, becomes negligible on experimental time scales. The high T-high H FM phase is then frozen-in. We accordingly postulate that below a certain temperature $T_K(H)$ the kinetics of the FM–AFM transformation is hindered and arrested just like in a quenched metglass. This is similar to observations at high pressures where the high density phase cannot transform[49] to the low density phase below a certain T_K, with T_K rising as the pressure rises. Metastable state thus obtained will have qualitatively different features from the usual phase-coexistence regime expected across the disorder-influenced first order transition. Preliminary studies on magnetocaloric material Gd_5Ge_4 have brought out this difference in 'end point memory effect' and in magnetic relaxation studies[50] and further study is in progress.

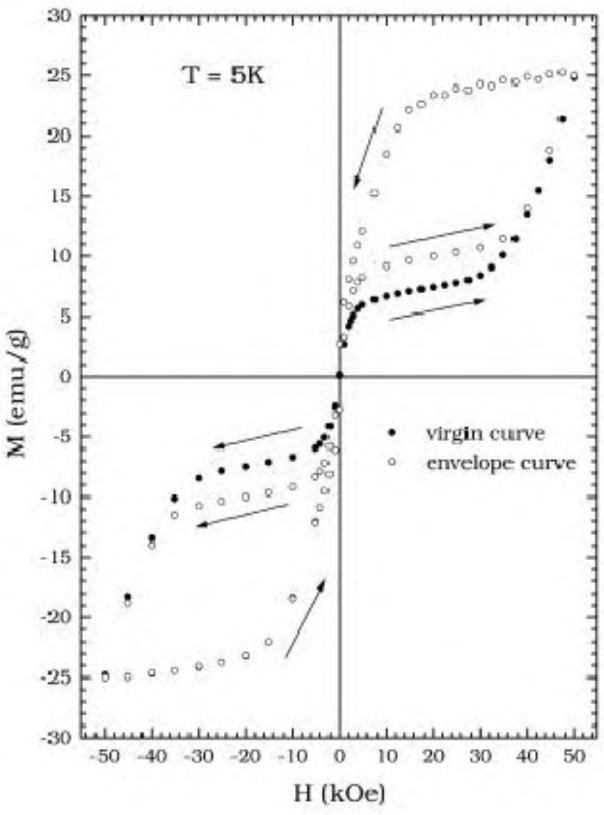

Figure 5. M vs H plots of Ce $(Fe_{0.96}Al_{0.04})_2$ obtained after cooling in zero field at $T = 5$ K. Note that the virgin M–H curve lies outside the envelope M–H curve. To confirm this anomalous nature of virgin curve we have also drawn this in the negative field direction after zero field cooling the sample[36].

While the above discussion on first order magneto-structural transition is confined to FM–AFM transition only, the other types of magnetic transitions from paramagnet (PM) to FM or between two FM states can be included within the same framework of understanding without losing generality. In fact the idea of phase-coexistence and metastability has already been proposed across the first order PM-FM transition in various Mn-oxide systems[51,52]. Similarly magneto-structural transition in other classes of magnetocaloric materials[53,54] and magnetic shape memory alloys[55] also involve a FOPT process and the role of this FOPT in the functionality of the concerned materials is recognized[53,55]. Further, epitaxial films of MnAs (which is a promising spintronics material) show an interesting first order magneto-structural transition[6,56]. The coexistence of ferromagnetic α-MnAs and paramagnetic β-MnAs phases in a wide temperature region appears to be a violation of Gibbs phase rule at first sight and is resolved by the presence of long-range elastic interaction in this strained heteroepitaxial film[6,56].

The idea of a disorder influenced first order transition has earlier been adopted in the study of ferroelectrics[57]. In recent times, an analogy has been drawn between various features observed in Mn-oxides and relaxor ferroelectrics. In these latter systems, electric field annealing and ageing effect have been observed which are compared with similar magnetic field-induced effects observed in Mn-oxides[18].

Outlook

Through our experimental studies on a test bed magnetic system namely $CeFe_2$ alloys, and comparing the results with CMR-Mn-oxide systems and Gd_5Ge_4 magnetocaloric material, we highlight the fact that phase-coexistence and

metastability associated with the magneto-structural transition in various materials are universal characteristics of a disorder-influenced FOPT. Comparing further with the rough landscape picture of the vortex solid melting transition[46] our observation shows the generality of the phase-coexistence phenomenon. Such a generality may even be stretched to encompass the ferroelectric materials[57]. This is likely to have interesting implications in multiferroic materials with interplay between magnetism and ferroelectricity[58]. We have highlighted certain anomalous features in various materials mentioned above pointing towards the interesting kinetics of the FOPT process. The role of this magneto-structural transition in the functionality of various classes of materials is also recognized. Further, the nucleation and growth process across a displacive structural transition is an area of current research interest[59] and we believe that present activities will add to the understanding of physical properties of various materials mentioned above and tuning their functionality.

It will not be out of context to point out that apart from highlighting various interesting aspects associated with the magneto-structural transitions in various functional materials, a relatively simple magnetic system like $CeFe_2$ provides an excellent context for experimental study of first order transition processes in general. It is far easier to explore H–T phase space than to use pressure as a variable. With appropriate experimental probes and samples with controlled disorder, it will be possible to study the generalized phenomena of nucleation (heterogeneous versus homogeneous) and growth kinetics in first order transition processes, and also their possible path dependence in the phase space defined in terms of the control variables. This subject of nucleation and growth in a FOPT continues to draw much attention because of its obvious impact in various fields[60].

1. Rao, C. N. R. and Raveau, B. (eds), *Colossal Magnetoresistance, Charge Ordering and Related Properties of Manganese Oxides*, World Scientific, Singapore, 1998.
2. Dagotto, E. *et al.*, *Phys. Rep.*, 2001, **344**, 1; Dagotto, E., *Nanoscale Phase Separation and Colossal Magneto-resistance*, Springer, New York, 2002.
3. Pecharsky, V. K. and Gschneidner Jr. K. A., *Adv. Mater.*, 2001, **13**, 683.
4. Pecharsky, V. K. *et al.*, *Phys. Rev. Lett.*, 2003, **91**, 197204.
5. Tang, H. *et al.*, *Phys. Rev.*, 2004, **B69**, 064410, and references therein.
6. Kaganer, V. M. *et al.*, *Phys. Rev. Lett.*, 2000, **85**, 341.
7. Imry, Y. and Wortis, M., *Phys. Rev.*, 1979, **B19**, 3580.
8. Schiffer, P. E. *et al.*, *Phys. Rev. Lett.*, 1995, **B75**, 3336.
9. White, R. M. and Geballe, T. H., *Long Range Order in Solids*, Academic Press, New York, 1979.
10. Cheong, S.-W. and Chen, C. H., p. 241 of ref. 1.
11. Kuwahara, H. *et al.*, *Science*, 1995, **270**, 961.
12. Tokura, Y. *et al.*, *Phys. Rev. Lett.*, 1996, **76**, 3184.
13. Vogt, T. *et al.*, *Phys. Rev.*, 1996, **B54**, 15303.
14. Asamatsu, A. *et al.*, *Nature*, 1997, **388**, 50.
15. Mahendiran, R. *et al.*, *Phys. Rev. Lett.*, 1999, **82**, 2191.
16. Guha, A. *et al.*, *Phys. Rev.*, 2000, **B62**, 5320.
17. Ritter, C. *et al.*, *Phys. Rev.*, 2000, **B61**, R9229.
18. Kimura, T. *et al.*, *Phys. Rev. Lett.*, 1999, **83**, 3940.
19. Parisi, F. *et al.*, *Phys. Rev.*, 2001, **B63**, 144419.
20. Hardy, V. *et al.*, *Phys. Rev.*, 2004, **B69**, R020407.
21. Wu, T. and Mitchell, J. F., *Phys. Rev.*, 2004, **B69**, R100405.
22. Moreo, A. *et al.*, *Phys. Rev. Lett.*, 2000, **84**, 5568.
23. Burgy, J. *et al.*, *Phys. Rev. Lett.*, 2001, **87**, 277202.
24. Uehara, M. *et al.*, *Nature*, 1999, **399**, 560.
25. Zhang, L. *et al.*, *Science*, 2002, **298**, 805.
26. Podzorov, V. *et al.*, *Phys. Rev.*, 2001, **B64**, 140406.
27. Ahn, K. H. *et al.*, *Nature*, 2004, **428** 401.
28. Burgy, J. *et al.*, *Phys. Rev. Lett.*, 2004, **92**, 097202.
29. Dho, J. and Hur, N. H., *Phys. Rev.*, 2003, **B67**, 214414.
30. Roy, S. B. and Coles, B. R., *J. Phys., Condens. Matter*, 1989, **1**, 419.
31. Roy, S. B. and Coles, B. R., *Phys. Rev.*, 1989, **B39**, 9360.
32. Kunkel, H. P. *et al.*, *Phys. Rev.*, 1996, **B53**, 15099.
33. Kennedy, S. J. and Coles, B. R., *J. Phys., Condens. Matter*, 1990, **2**, 1213.
34. Manekar, M. A. *et al.*, *J. Phys., Condens. Matter*, 2000, **12**, L409.
35. Manekar, M. A. *et al.*, *J. Phys., Condens. Matter*, 2000, **12**, 9645.
36. Manekar, M. A. *et al.*, *Phys. Rev.*, 2001, **B64**, 104416.
37. Singh, K. J. *et al.*, *Phys. Rev.*, 2002, **B65**, 94419.
38. Chattopadhyay, M. K., *Phys. Rev.*, 2003, **B68**, 174404.
39. Sokhey, K. J. S. *et al.*, *Solid State Commun.*, 2004, **129**, 19.
40. Mydosh, J. A., *Spin Glasses*, Taylor & Francis, London, 1992.
41. Freitas, R. S. *et al.*, *Phys. Rev.*, 2002, **B65**, 104403.
42. Chaikin, P. M. and Lubensky, T. C., *Principles of Condensed Matter Physics*, Cambridge University Press, Cambridge, 1995.
43. Roy, S. B. and Chaddah, P., *Physica*, 1997, **C279**, 70; *J. Phys.: Condens. Matter*, 1997, **9**, L625.
44. Sokhey, K. J. S. *et al.* (unpublished).
45. Roy, M., Mitchell, J. F. and Schiffer, P., *J. Appl. Phys.*, 2000, **87**, 5831.
46. Soibel, A. *et al.*, *Nature*, 2000, **406**, 283.
47. Roy, S. B. *et al.*, *Phys. Rev. Lett.*, 2004, **92**, 147203.
48. Debenedetti, P. G., *Metastable Liquids*, Princeton University Press, Princeton, 1996.
49. Sharma, S. M. and Sikka, S. K., *Prog. Mater. Sci.*, 1996, **40**, 1.
50. Chattopadhyay, M. K. *et al.*, *Phys. Rev. B* (in press).
51. Biernacki, S. W., *Phys. Rev.*, 2003, **68**, 174417 (and references herein).
52. Raychaudhuri, A. K. (private communication).
53. Zhou, X. *et al.*, *J. Phys., Condens. Matter*, 2004, **16**, L39.
54. Liu, X. B. *et al.*, *J. Magn. Magn. Matr.*, 2004, **270**, 305.
55. Wang, W.-H. *et al.*, *Phys. Rev.*, 2001, **B65**, 012416.
56. Das, A. K. *et al.*, *Phys. Rev. Lett.*, 2003, **91**, 087203.
57. Schremmer, H. *et al.*, *Phys. Rev. Lett.*, 1989, **62**, 1896.
58. Hur, N. *et al.*, *Nature*, 2004, **429**, 392.
59. Klein, W. *et al.*, *Phys. Rev. Lett.*, 2002, **88**, 085701.
60. Cacciuto, A. *et al.*, *Nature*, 2004, **428**, 404.

ACKNOWLEDGEMENTS. It is a pleasure to acknowledge fruitful scientific collaborations with M. A. Manekar, M. K. Chattopadhyay, S. Chaudhary, K. J. S. Sokhey, A. K. Nigam, G. Perkins, Y. Bugoslavsky and L. F. Cohen.